Published for SISSA by Springer

Received: *December 2, 2024*
Accepted: *January 24, 2025*
Published: *February 28, 2025*

From G_2 to SO(8): Emergence and reminiscence of supersymmetry and triality

Zhi-Qiang Gao[a] **and Congjun Wu**[b,c,d,e,*]

[a] *Department of Physics, University of California, Berkeley, California 94720, U.S.A.*
[b] *New Cornerstone Science Laboratory, Department of Physics, School of Science, Westlake University, Hangzhou 310024, Zhejiang, China*
[c] *Institute for Theoretical Sciences, Westlake University, Hangzhou 310024, Zhejiang, China*
[d] *Key Laboratory for Quantum Materials of Zhejiang Province, School of Science, Westlake University, Hangzhou 310024, Zhejiang, China*
[e] *Institute of Natural Sciences, Westlake Institute for Advanced Study, Hangzhou 310024, Zhejiang, China*

E-mail: zqgao@berkeley.edu, wucongjun@westlake.edu.cn

Abstract: We construct a (1+1)-dimension continuum model of 4-component fermions incorporating the exceptional Lie group symmetry G_2. Four gapped and five gapless phases are identified via the one-loop renormalization group analysis. The gapped phases are controlled by four different stable SO(8) Gross-Neveu fixed points, among which three exhibit an emergent triality, while the rest one possesses the self-triality, i.e., invariant under the triality mapping. The gapless phases include three SO(7) critical ones, a G_2 critical one, and a Luttinger liquid. Three SO(7) critical phases correspond to different SO(7) Gross-Neveu fixed points connected by the triality relation similar to the gapped SO(8) case. The G_2 critical phase is controlled by an unstable fixed point described by a direct product of the Ising and tricritical Ising conformal field theories with the central charges $c = \frac{1}{2}$ and $c = \frac{7}{10}$, respectively, while the latter one is known to possess spacetime supersymmetry. In the lattice realization with a Hubbard-type interaction, the triality is broken into the duality between two SO(7) symmetries and the supersymmetric G_2 critical phase exhibits the degeneracy between bosonic and fermionic states, which are reminiscences of the continuum model.

Keywords: Field Theories in Lower Dimensions, Higher Spin Symmetry, Renormalization Group, Supersymmetry and Duality

ArXiv ePrint: 2411.08107

*Corresponding author.

https://doi.org/10.1007/JHEP02(2025)202

JHEP02(2025)202

Contents

1 Introduction

Exceptional Lie groups play an essential role in the study of modern condensed matter physics [1–4]. E_8, the largest exceptional Lie group, is employed to describe an exotic quantum Hall state [5]. The E_8 excitations are also observed in an anti-ferromagnetic Ising spin chain [2]. On the other hand, the smallest exceptional Lie group G_2 with rank-2 and 14 dimensional [6], which is the automorphism group of the non-associative algebra octonion [7], has especially attracted many interests recently [8–11]. In particular, a lattice model which has an explicit G_2 symmetry based on 4-component, such as spin-$\frac{3}{2}$, fermions is constructed [9]. However, G_2 symmetry is shown to be intrinsically strongly correlated, that it cannot be realized in non-interacting systems [9], which makes it hard to study analytically.

Inspired by ref. [12], we investigate the coarse-grained version of the lattice G_2 model [9] in (1+1) spacetime dimension, where many powerful tools can be utilized to study strong correlation systems. Through an one-loop renormalization group (RG) calculation, we reveal the hidden SO(8) triality structure. The phase diagram is consistent with the mean-field analysis in the lattice model [9]. Interestingly, we also find in the phase diagram that one critical phase is described by the tricritical Ising (TCI) conformal field theory (CFT) [13]. TCI CFT actually has spacetime supersymmetry [14, 15], which is corresponding to the degeneracy between bosonic and fermionic states in the lattice model [9]. Coset constructions based on

JHEP02(2025)202

G_2 Wess-Zumino-Witten (WZW) models realizing exotic non-Abelian statistics [8, 10, 11] can also emerge in our model. Moreover, our model also exhibits the exotic phenomena of multiversality and unnecessary criticality [16, 17].

The rest part of this article is organized as follows: in section 2, the models are introduced both in the form of the lattice Hamiltonian and in the coarse-grained continuum version. In section 3, the one-loop RG analyses are perform to yield the RG flow patterns and the corresponding gapped and critical phases. The embedding of the lattice model in the phase diagram of the continuum model is presented in section 4. Conclusions are presented in section 5.

2 The model Hamiltonians

2.1 The minimal G_2 symmetric lattice model

In a preceding work [9], we construct a minimal lattice model with the G_2 symmetry based on 4-component spin-$\frac{3}{2}$ fermions as briefly reviewed below. The 4-component spinor $\psi_\sigma(i)$ defined on each site i with $\sigma = \pm\frac{3}{2}, \pm\frac{1}{2}$ spans a local SO(8) algebra $\{N_{ab}(i)\}$ with $0 \le a, b \le 7$ [9, 18, 19]. Here each generator $N_{ab}(i)$ is a fermion bilinear operator in the particle-hole or particle-particle channel.

An SO(5), or, isomorphically, Sp(4) subalgebra of SO(8) is simply $L_{ab} = N_{ab} = \frac{1}{2}\psi^\dagger(i)\Gamma_{ab}\psi(i)$ with $1 \le a, b \le 5$, where Γ_{ab}'s are the commutators among the five rank-2 anti-commuting Γ-matrices, i.e., $\Gamma_{ab} = \frac{i}{2}[\Gamma_a, \Gamma_b]$ with $\{\Gamma_a, \Gamma_b\} = 2\delta_{ab}$. The 10 generators of Sp(4) unify both spin and spin-octupole operators based on the spin-$\frac{3}{2}$ spinor ψ. An SO(7) subalgebra, denoted as SO(7)$_A$ below, is an extension of Sp(4), defined as $M_{ab}(i) = N_{ab}(i)$ with $0 \le a, b \le 6$. It further includes, and hence, unifies the particle number $M_{06}(i) = \frac{1}{2}(\psi^\dagger(i)\psi(i) - 2)$, and the pairing operators in the spin quintet channel $M_{0a}(i) = \frac{1}{2}\psi^\dagger(i)\Gamma_a R\psi^\dagger(i)$ with $1 \le a \le 5$ where R is the charge conjugation matrix satisfying $R^{\mathbf{T}} = R^{-1} = -R$. Pairing operators are complex, and one complex operator is equivalent to two real ones. The rest 7 operators denoted $V_a(i) = N_{a7}(i)$ form a vector representation of the SO(7)$_A$ defined above, unifying 5 spin quadrupole operators with $N_{a7} = \frac{1}{2}\psi^\dagger(i)\Gamma^a\psi_(i)$ with $1 \le a \le 5$ and 1 complex singlet pairing operator $N_{07} = \psi^\dagger(i)R\psi^\dagger(i)$. For details please refer to appendix A.

The SO(7)$_A$ algebra defined above can be decomposed into a 14-dimensional G_{ab} part spanning the G_2 subalgebra and a 7-vector T_a belonging to the coset SO(7)$_A/G_2$ defined as [9]

$$G_{ab}(i) = \frac{2}{3}M_{ab}(i) + \frac{1}{6}C_{abcd}M_{cd}(i), \quad T_a(i) = \frac{1}{2\sqrt{3}}C_{abc}M_{bc}(i), \tag{2.1}$$

where C_{abcd} is the structure constant of the non-associative octonion algebra. Note that $G_{ab}(i)$ satisfy 7 constraints $C_{abc}G_{ab}(i) = 0$, where $C_{abc} = \frac{1}{24}\epsilon_{abcdefg}C_{defg}$ is the dual tensor of C_{abcd}. Therefore, only 14 of them are linear independent. $T_a(i)$ transform under the vector representation of G_2 [9, 20]. $V_a(i)$ defined before also form a G_2 vector representation [9, 20]. Inversely, the SO(7)$_A$ generators can be represented by $G_{ab}(i)$ and $T_a(i)$ as

$$M_{ab}(i) = G_{ab}(i) + \frac{1}{\sqrt{3}}C_{abc}T_c(i). \tag{2.2}$$

Another SO(7) algebra denoted as $\mathrm{SO}(7)_B$ is constructed below sharing the same G_2 subalgebra as in $\mathrm{SO}(7)_A$. Define operators $T'_a(i)$ and $V'_a(i)$ as a "120° rotation" of $T_a(i)$ and $V_a(i)$:

$$T'_a(i) + iV'_a(i) = e^{i\frac{2}{3}\pi}(T_a(i) + iV_a(i)). \tag{2.3}$$

The generators of $\mathrm{SO}(7)_B$ are expressed as [9],

$$M'_{ab}(i) = G_{ab}(i) + \frac{1}{\sqrt{3}} C_{abc} T'_c(i), \tag{2.4}$$

and $V'_a(i)$ form an vector representation of $\mathrm{SO}(7)_B$. The Casimirs of these two SO(7)'s are connected by the duality relations [9],

$$\begin{aligned} C_A(i) &= \sum_{0\le a<b\le 6} M_{ab}(i)M_{ab}(i) = \frac{1}{4}\sum_{abcd} C_{abcd} M'_{ab}(i)M'_{cd}(i), \\ C_B(i) &= \sum_{0\le a<b\le 6} M'_{ab}(i)M'_{ab}(i) = \frac{1}{4}\sum_{abcd} C_{abcd} M_{ab}(i)M_{cd}(i). \end{aligned} \tag{2.5}$$

A lattice model $H = H_0 + H_{\mathrm{int}}^{G_2}$ realizing the G_2 symmetry has been constructed as the intersection between $\mathrm{SO}(7)_A$ and $\mathrm{SO}(7)_B$ symmetries [9],

$$\begin{aligned} H_0 &= -t_{\mathrm{hop}} \sum_{\langle ij\rangle,\sigma} \left(\psi^\dagger_\sigma(i)\psi_\sigma(j) + h.c.\right), \\ H_{\mathrm{int}}^{G_2} &= u\sum_i C_A(i) + v\sum_i C_B(i), \end{aligned} \tag{2.6}$$

where u and v are coupling constants. When $v = 0$, or, $u = 0$, the lattice model of (2.6) restores the $\mathrm{SO}(7)_A$, or, $\mathrm{SO}(7)_B$ symmetry, respectively.

Besides the $\mathrm{SO}(7)_A$ and $\mathrm{SO}(7)_B$ symmetries in the lattice model of (2.6), there exists a third $\mathrm{SO}(7)_M$ one sharing the same G_2 sub-group, where M stands for Majorana. Its generators $M''_{ab}(i)$ can be similarly defined through (2.4), with $T'_a(i)$ and V'_a substituted by $T''_a(i)$ and V''_a defined by "$-120°$ rotation", i.e., $T''_a(i) + iV''_a(i) = e^{-i\frac{2}{3}\pi}(T_a(i) + iV_a(i))$. The $\mathrm{SO}(7)_M$ algebra can be naturally expressed in terms of Majorana fermions constructed based on the 4-component spinor $\psi_\sigma(i)$, i.e., $\chi_m(i)$ with $0 \le m \le 7$ (see appendix A for a detailed definition). By straightforward calculations, we express M''_{ab} and $V''_a(i)$ as

$$M''_{ab}(i) = i\chi_m(i)\chi_n(i), \quad V''_a(i) = i\chi_0(i)\chi_m(i), \tag{2.7}$$

where $1 \le m \le 7$. As $(i\chi_m(i)\chi_n(i))^2$ is always equal to 1, the Casimir of $\mathrm{SO}(7)_M$ is a c-number. Therefore, it is absent in the lattice Hamiltonian (2.6) where the on-site Hubbard-type interactions are written in terms of Casimirs. Nevertheless, in the coarse-grained continuum model, the $\mathrm{SO}(7)_M$ symmetry will emerge at low energy and fulfill the SO(8) triality relation.

2.2 The coarse-grained continuum model in (1+1)D

In (1+1)D, the low energy effective theory of the free Hamiltonian H_0 in (2.6) is the $\mathrm{SO}(8)_1$ WZW model [21] expressed in terms of Majorana fields $\chi_m^{R/L}$ with $0 \le m \le 7$. These

Majorana fields $\chi_m(i)$ defined above form the 8-dimensional vector representation of the SO(8) symmetry. The disorder operators of the $\mathrm{SO}(8)_1$ WZW model build another two sets of Majorana fermions spanning the 8-dimensional spinor and anti-spinor representations [21]. Hence, when the SO(8) symmetry is broken to SO(7), three different choices are possible such that one of the three 8-dimensional representations is decomposed to $8 = 7 \oplus 1$ under the SO(7) while the other two remain 8-dimensional. If this residual SO(7) symmetry is chosen to be $\mathrm{SO}(7)_M$, then χ_0 is the singlet invariant under $\mathrm{SO}(7)_M$, and $\chi_{1,2,\ldots,7}$ form the 7-dimensional vector of $\mathrm{SO}(7)_M$. The triality relation among the three 8-dimensional SO(8) representations is inherited by that among SO(7) symmetries.

The chiral currents $G_{ab}^{R/L}$, $T_a^{R/L}$, and $V_a^{R/L}$ in the coarse-grained model are defined as fermion bilinears similar to their lattice cousins, with $\psi_\sigma(i)$ substituted by $\psi_{R,\sigma}(z)$ and $\psi_{L,\sigma}(\bar{z})$ for the right- and left-moving fermions, respectively. Note that Umklapp terms $\psi_R^\dagger \psi_R^\dagger \psi_L \psi_L$ and $\psi_L^\dagger \psi_L^\dagger \psi_R \psi_R$ (spin indices omitted) are allowed, since H_0 should be at half-filling to maintain the G_2 symmetry. Any linear combination of T_a and V_a form a G_2 vector. Therefore, in terms of $\mathrm{SO}(7)_A$ operators, the most general form of the G_2 invariant low energy effective Hamiltonian density reads

$$\mathcal{H}_{\text{int}} = g \sum_{a \neq b} G_{ab}^R G_{ab}^L + t \sum_a T_a^R T_a^L + y \sum_a V_a^R V_a^L + \frac{w}{\sqrt{2}} \sum_a \left(T_a^R V_a^L + V_a^R T_a^L \right), \tag{2.8}$$

where g, t, y, and w are coupling constants. The $\mathrm{SO}(7)_A$ symmetry appears at $w = 0$, $t = 2g$, and y arbitrary.

To explicitly reveal the triality relation, the Hamiltonian density (2.8) is rewritten in an equivalent way as

$$\mathcal{H}_{\text{int}} = g \sum_{a \neq b} G_{ab}^R G_{ab}^L + t_A \sum_a T_a^R T_a^L + t_B \sum_a T_a'^R T_a'^L + t_M \sum_a T_a''^R T_a''^L, \tag{2.9}$$

with the relation

$$t_A = t - \frac{1}{3} y, \quad t_B = \frac{2}{3} y + \frac{\sqrt{6}}{3} w, \quad t_M = \frac{2}{3} y - \frac{\sqrt{6}}{3} w. \tag{2.10}$$

The triality of the three SO(7) symmetries is already implied in the permutation of three coupling constants t_A, t_B, and t_M.

3 Renormalization group flows and fixed planes

Based on the G_2 current algebra [20], we perform the one-loop RG calculation in appendix B, yielding the following RG equations for the coupling constants defined in (2.8),

$$\begin{aligned}
\frac{\mathrm{d}g}{\mathrm{d}l} &= 16g^2 + t^2 + y^2 + w^2, \\
\frac{\mathrm{d}t}{\mathrm{d}l} &= 16gt + 2t^2 + 2y^2 - 2w^2, \\
\frac{\mathrm{d}y}{\mathrm{d}l} &= 16gy + 4ty + 2w^2, \\
\frac{\mathrm{d}w}{\mathrm{d}l} &= 16gw - 4tw + 4yw.
\end{aligned} \tag{3.1}$$

For illustrating of the triality explicitly, the RG equations (3.1) can be cast in terms of g and t_i with $i \in \{A, B, M\}$ in a more symmetric form as

$$\begin{aligned} \frac{\mathrm{d}g}{\mathrm{d}l} &= 16g^2 + \sum_i t_i^2 + \frac{1}{4}\sum_{i\neq j} t_i t_j, \\ \frac{\mathrm{d}t_i}{\mathrm{d}l} &= 16 g t_i + 2t_i^2 + 4\frac{t_A t_B t_M}{t_i}. \end{aligned} \tag{3.2}$$

An analytical solution to the RG equations (3.2) would be difficult, however, the geometrical structure of the RG flows is rather clear. They exhibit fixed planes (not necessarily the same as critical surfaces) in which the RG flows keep in-plane evolutions. The fixed planes can be classified into two types, the SO(7) symmetric and the G_2 critical, respectively, as discussed below.

3.1 The SO(7) symmetric fixed planes

There exist three planes in which the G_2 symmetry is enlarged to the $\mathrm{SO}(7)_A$, $\mathrm{SO}(7)_B$, and $\mathrm{SO}(7)_M$ symmetries, respectively. They are related to each other by the triality relation as well as the RG flow patterns. The RG equations with SO(7) symmetry have been investigated in literature [22, 23]. For the self-contentedness of this work, we summarize the corresponding stable and critical quantum phases.

For an SO(7) plane, the coupling constants satisfy the following relation,

$$\mathrm{SO}(7)_i \text{ symmetric fixed plane } P_i: \; t_j = t_k = 4g - 2t_i, \tag{3.3}$$

where $\{i, j, k\}$ are permutations of $\{A, B, M\}$. Within these SO(7) fixed planes, the RG equations can be solved analytically. The resulting fixed points (flows) characterize different quantum phases and phase transitions.

Taking the plane of P_A as an example, the $\mathrm{SO}(7)_A$ symmetry is explicit as seen from the reduced interaction Hamiltonian density,

$$\mathcal{H}_A = g \sum_{a\neq b} M_{ab}^R M_{ab}^L + y \sum_a V_a^R V_a^L. \tag{3.4}$$

The RG equations in the $\mathrm{SO}(7)_A$ symmetric plane P_A are reduced to

$$\frac{\mathrm{d}g}{\mathrm{d}l} = 20g^2 + y^2, \quad \frac{\mathrm{d}y}{\mathrm{d}l} = 24gy. \tag{3.5}$$

The solutions to RG equations (3.5) can be classified in the following cases.

Case (I): *The fully gapped SO(8) Gross-Neveu (GN) phases.* There exists a stable SO(8) GN [24] fixed flow characterized by the interaction paramter set of $y = t = 2g \to +\infty$ and $w = 0$, or, equivalently, $t_A = t_B = t_M = \frac{4}{3}g \to +\infty$. The Hamiltonian density along this line is reduced to

$$\mathcal{H}_{\mathrm{GN}}^{\mathrm{SO}(8)} = g \sum_{a\neq b} M_{ab}^R M_{ab}^L + 2g \sum_a V_a^R V_a^L = g \sum_{a\neq b} N_{ab}^R N_{ab}^L, \tag{3.6}$$

which describes the fully gapped SO(8) GN phase. This fixed flow is at the intersection of three $\mathrm{SO}(7)_i$ fixed planes with $i \in \{A, B, M\}$ and is invariant under the permutation of t_i. Therefore, it exhibits SO(8) self-triality.

Another SO(8) phase is also stable characterized by the fixed point of $y = -t = -2g \to -\infty$ and $w = 0$, or, equivalently, $t_B = t_M = -\frac{1}{2}t_A = -\frac{4}{3}g \to -\infty$. Along this line, the interaction Hamiltonian density is reduced to

$$\mathcal{H}_{\mathrm{GN}}^{\mathrm{SO}(8)_A} = g \sum_{a \neq b} M_{ab}^R M_{ab}^L - 2g \sum_a V_a^R V_a^L. \tag{3.7}$$

It is related to the previous SO(8) phase of (3.6) by the chiral transformation [21, 23] which keeps the current of left-movers but change that of right-movers to $\{M_{ab}^R, -V_a^R\}$. Such a phase is also fully gapped denoted as the $\mathrm{SO}(8)_A$ GN phase.

Case (II): *The critcal SO(7) GN phase.* This phase is controlled by the unstable SO(7) GN fixed flow characterized by $t = 2g \to +\infty$ and $y = w = 0$, or, equivalently, $t_B = t_M = 0$, $t_A = 2g \to +\infty$. Along this flow, the interaction Hamiltonian density is reduced to

$$\mathcal{H}_{\mathrm{GN}}^{\mathrm{SO}(7)_A} = g \sum_{a \neq b} M_{ab}^R M_{ab}^L. \tag{3.8}$$

In such a state, 7 Majorana modes are gapped out by the GN-type interaction while 1 Majorana mode remains gapless [23, 25]. It describes a critical phase with the $\mathrm{SO}(7)_A$ symmetry, sandwiched by two gapped SO(8) phases discussed previously. This critical phase, denoted as the $\mathrm{SO}(7)_A$ GN phase, has the central charge of $c = \frac{1}{2}$ attributed to the gapless Majorana mode, yielding a phase transition in the Ising universality class. The two gapped SO(8) phases are Ising dual to each other.

Case (III): *The critical $SO(8)_1$ WZW phase.* This phase is characterized by the unstable fixed point of $g = t = y = w = 0$, or, equivalently, $g = t_A = t_B = t_M = 0$. Its central charge $c = 4$ corresponding to the free theory of 8 Majoranas, i.e., the $\mathrm{SO}(8)_1$ WZW model. It controls the gapless Luttinger liquid phase. Apparently, this fixed point also exhibits self-triality.

Due to the triality, RG flows and the stable phases of the $\mathrm{SO}(7)_B$ and $\mathrm{SO}(7)_M$ symmetric fixed planes should exhibit the same structure as the case of $\mathrm{SO}(7)_A$. Hence, three $\mathrm{SO}(8)_i$ $(i = A, B, M)$ gapped phases are related to each other by the triality. The phase transitions between the gapped SO(8) GN phase and $\mathrm{SO}(8)_i$ GN phases are in the Ising universality class with central charge $c = \frac{1}{2}$, controlled by $\mathrm{SO}(7)_i$ GN fixed flows. The three $\mathrm{SO}(7)_i$ GN points, as well as the three critical Ising phases are also related to each other by the triality relation.

The schematic RG flows and the phase diagram on the $\mathrm{SO}(7)_A$ symmetric fixed plane P_A are shown in figure 1. By substituting the subscript A by B/M, the similar physics appears on $\mathrm{SO}(7)_{B/M}$ symmetric fixed planes. The lattice model (2.6) with $v = 0$ possesses the $\mathrm{SO}(7)_A$ symmetry. As varying u, its phase evolution is also marked in figure 1. In appendix C, we provide a standard bosonization analysis [21–23, 26], which gives rise to the same phase diagram.

JHEP02(2025)202

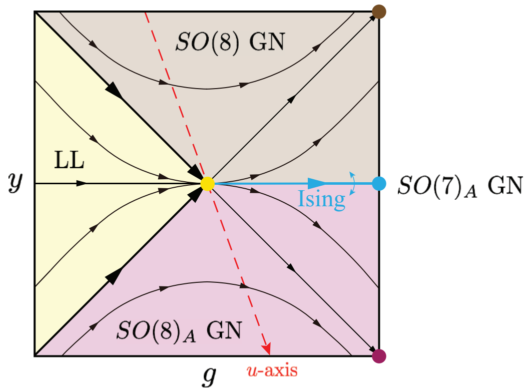

Figure 1. The RG flows and phase diagram on the $\mathrm{SO}(7)_A$ symmetric fixed plane. The horizontal and vertical axes are labeled by g and y, respectively. Phase boundaries are marked by thick lines. The SO(8) GN, $\mathrm{SO}(8)_A$ GN, and $\mathrm{SO}(7)_A$ GN fixed points (defined as $g \to +\infty$ points of the fixed flows) are marked by brown, blue, and crimson dots, respectively. The yellow dot stands for the free Majorana fixed point. "LL" denotes the Luttinger liquid phase. The transition between the SO(8) GN phase and the $\mathrm{SO}(8)_A$ GN phase is described by the critical $\mathrm{SO}(7)_A$ GN phase in the Ising universality class. Phase structures in the $\mathrm{SO}(7)_{B/M}$ fixed planes can be obtained via the triality mapping. The embedding of the u-axis in the lattice model phase diagram is colored in red.

3.2 The G_2 critical fixed planes

Aside from the GN-type fixed flows discussed above, the RG equations (3.1) have an unstable flow away from all the three SO(7) symmetric fixed planes. This G_2 symmetric fixed flow is characterized by $g \to +\infty$ and $t = y = w = 0$, or, equivalently, $g \to +\infty$, $t_A = t_B = t_M = 0$, which exhibits the self-triality. The corresponding interaction Hamiltonian density reads,

$$\mathcal{H}_{\mathrm{TCI}}^{G_2} = g \sum_{a \neq b} G_{ab}^R G_{ab}^L. \tag{3.9}$$

Interestingly, $g \to +\infty$ does not completely gap out the spectra, but results in a tricritical Ising (TCI) phase [8, 13] with central charge $c = \frac{7}{10}$. The emergent symmetry of this critical phase is not only G_2, but also the $\mathcal{N} = 1$ spacetime supersymmetry inherited from the TCI CFT [14, 15].

In the Majorana basis, (3.9) contains only 7 of the 8 Majorana modes, and the decoupled one χ_0 remains gapless. Hence, the total central charge is $c = \frac{7}{10} + \frac{1}{2} = \frac{6}{5}$. A CFT with such a central charge has a parafermion representation [27–29], which may be realized on the edge of certain fractional quantum Hall states [28, 29]. It remains an interesting question whether some quantum Hall bilayer systems could host this model on the edge through certain modifications such as edge reconstructions [30–32]. In addition, (3.9) realizes the model proposed in ref. [8] for topological superconducting edge states which exhibit non-Abelian Fibonacci anyonic properties. The model of (2.8) could be viewed as a generalization of their case.

The G_2 TCI fixed flow is special. We can pick up any one GN-type fixed flow together with the G_2 TCI one to form a fixed plane. Consider the interaction Hamiltonian density on such a plane. It can be rearranged as

$$\mathcal{H}_{\mathrm{critical}}^{G_2} = \tilde{g} \sum_{a \neq b} G_{ab}^R G_{ab}^L + \tilde{n} \sum_{a \neq b} \tilde{N}_{ab}^R \tilde{N}_{ab}^L, \tag{3.10}$$

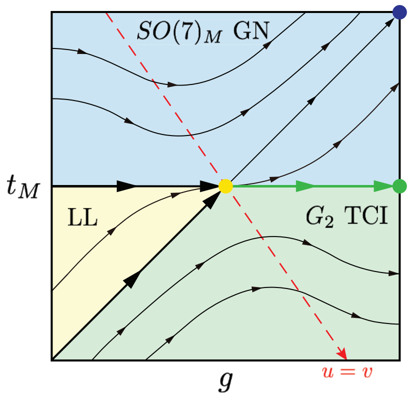

Figure 2. The RG flows and phase diagram on the G_2 critical fixed planes spanned by the G_2 TCI fixed flow and the $\mathrm{SO}(7)_M$ critical GN fixed flow. The horizontal and vertical axes are labeled by g and t_M, respectively. The $\mathrm{SO}(7)_M$, G_2 TCI, and free Majorana fixed points are denoted by the indigo, green, and yellow dots, respectively. Phase structures in other G_2 critical fixed planes are similar. The embedding of the $u = v$ line in the lattice model is colored in red.

where $\tilde{N}_{ab}$ are the generators of the emergent symmetry on the GN fixed flow. For example, for the $\mathrm{SO}(8)_A$ GN fixed flow, $\{\tilde{N}^R_{ab}\} = \{M^R_{ab}, -V^R_c\}$ and $\{\tilde{N}^L_{ab}\} = \{M^L_{ab}, V^L_c\}$ are generators of the $\mathrm{SO}(8)_A$ symmetry. Since the emergent symmetry is enlarged including the G_2 as a subgroup, the closure of Lie algebra ensures the RG flow to remain in-plane. The corresponding fixed points (flows) and phases are the GN fixed flow controlling the gapped or critical phase with emergent symmetry, the G_2 TCI fixed flow controlling the G_2 TCI phase, and the free Majorana fixed point contronlling the Luttinger liquid phase. As an example, we choose the GN fixed flow as the $\mathrm{SO}(7)_M$ critical one. Correspondingly the fixed plane has $t_A = t_B = 0$, on which the RG equations are reduced to

$$\frac{\mathrm{d}g}{\mathrm{d}l} = 16g^2 + t_M^2, \quad \frac{\mathrm{d}t_M}{\mathrm{d}l} = 16gt_M + 2t_M^2. \tag{3.11}$$

It indeed possesses the $\mathrm{SO}(7)_M$ critical fixed flow of $t_A = t_B = 0$ and $t_M = 2g \to +\infty$, or, equivalently, $t = \frac{1}{3}y = -\frac{1}{\sqrt{6}}w = \frac{1}{2}g \to +\infty$. Along the $\mathrm{SO}(7)_M$ critical flow, the interaction Hamiltonian density is reduced to

$$\begin{aligned}\mathcal{H}_{\mathrm{GN}}^{\mathrm{SO}(7)_M} &= g\sum_{a\neq b} G^R_{ab}G^L_{ab} + \frac{g}{2}\sum_a T^R_a T^L_a + \frac{3g}{2}\sum_a V^R_a V^L_a - \frac{\sqrt{3}g}{2}\sum_a \left(T^R_a V^L_a + V^R_a T^L_a\right) \\ &= g\sum_{a\neq b} M''^R_{ab} M''^L_{ab}.\end{aligned} \tag{3.12}$$

The schematic RG flows and the phase diagram on this G_2 critical fixed planes are shown in figure 2. A complete list of fixed flows is given in table 1.

3.3 Phase diagrams in fixed bodies

The transitions between the SO(8) GN phase and each of the $\mathrm{SO}(8)_i$ GN phase is revealed by the Ising duality in the corresponding SO(7) fixed plane. Nevertheless, phase transitions between any two of these three $\mathrm{SO}(8)_i$ GN phases are more involved, since different stable

t_A/g	t_B/g	t_M/g	Symmetry	Fixed plane
4/3	4/3	4/3	SO(8)	$P_A,\ P_B,\ P_M$
8/3	−4/3	−4/3	$\mathrm{SO}(8)_A$	P_A
2	0	0	$\mathrm{SO}(7)_A$	P_A
−4/3	8/3	−4/3	$\mathrm{SO}(8)_B$	P_B
0	2	0	$\mathrm{SO}(7)_B$	P_B
−4/3	−4/3	8/3	$\mathrm{SO}(8)_M$	P_M
0	0	2	$\mathrm{SO}(7)_M$	P_M
0	0	0	G_2 SUSY	Any

Table 1. Fixed flows ($g \neq 0$), the associated symmetries, and the corresponding fixed planes. P_i ($i = A, B, M$) represents the $\mathrm{SO}(7)_i$ symmetric fixed plane. The G_2 TCI fixed flow has emergent supersymmetry endowed by the TCI CFT. In the last row, "Any" means a plane spanned by the G_2 TCI fixed flow and anyone of the GN fixed flows is a fixed plane.

GN fixed flows are not in the same fixed plane. To investigate this problem, we find the following relation based on the RG equations (3.2),

$$\frac{\mathrm{d}\tilde{t}}{\mathrm{d}l} = 16g\tilde{t}, \tag{3.13}$$

with $\tilde{t} = t_A + t_B + t_M$. Hence, during the evolution $\tilde{t} = 0$ is maintained. The fixed body spanned by g and $\tilde{t} = 0$ includes all the three $\mathrm{SO}(8)_i$ GN fixed flows exhibiting the triality.

The phase diagram in fixed body $\tilde{t} = 0$ is shown in figure 3(a), which exhibits the D_3 symmetry as a consequence of the triality among the three $\mathrm{SO}(8)_i$ phases. The G_2 TCI fixed flow and the free Majorana fixed point also lie in this fixed body, as indicated in table 1. The phase diagram shows that the transition between any two of the three $\mathrm{SO}(8)_i$ GN phases is described by either the Luttinger liquid phase with central charge $c = 4$, or, the G_2 TCI phase with central charge $c = \frac{6}{5}$, both of which are actually multi-critical. This coincides with the phenomenon of multiversality that the phase transitions between two phases can have more than one universality classes [16, 17].

The RG equations (3.2) also show that if any two of $t_A = t_B = t_M$ are equal, this relation is also maintained during the RG evolution. Hence, there exist another class of three fixed bodies given by $t_A = t_B$, $t_B = t_M$, and $t_M = t_A$, respectively, which are related by triality. As an example, the phase diagram in the fixed body $t_A = t_B$ is shown in figure 3(b), in which the $\mathrm{SO}(7)_M$ fixed plane P_M spanned by three GN fixed flows is embedded.

4 Embedding of the lattice model

Neither triality nor the spacetime supersymmetry survives in the 1D lattice Hubbard-type model of (2.6). It is natural to ask the reason behind such a loss. This is equivalent to investigate the embedding of the lattice model phase diagram into that of the continuum model. The phase diagram of the lattice Hamiltonian (2.6) is spanned by u- and v-axis, along which the $\mathrm{SO}(7)_A$ and $\mathrm{SO}(7)_B$ symmetries are restored, respectively. Therefore, the u/v-axis must be a straight line passing the origin point in the $\mathrm{SO}(7)_{A/B}$ fixed plane $P_{A/B}$ in the continuum model phase diagram.

JHEP02(2025)202

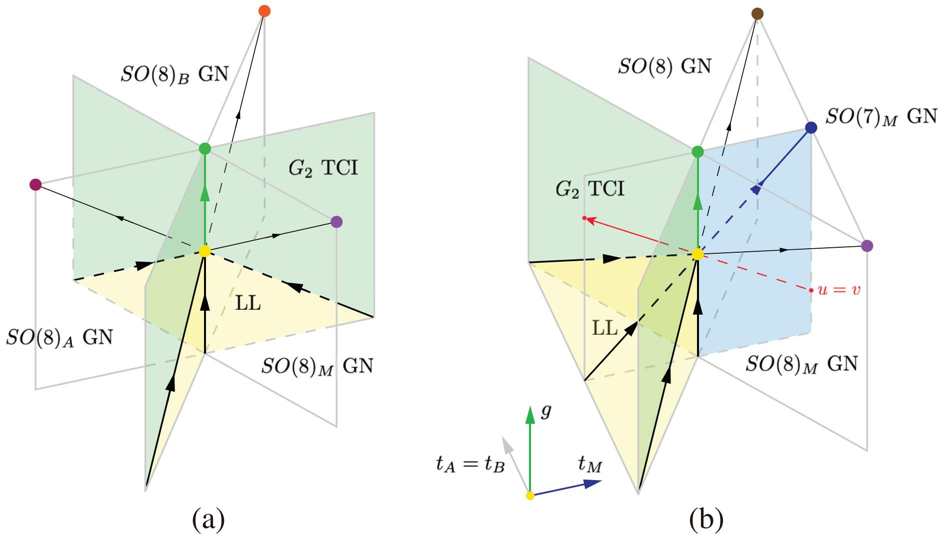

Figure 3. The phase diagrams in the fixed bodies (a) $\tilde{t} = t_A + t_B + t_M = 0$ and (b) $t_A = t_B$. The fixed flows are marked as arrows, and the critical surfaces are colored. In (a), $\mathrm{SO}(8)_A$ GN, $\mathrm{SO}(8)_B$ GN, $\mathrm{SO}(8)_M$ GN, G_2 TCI, and free Majorana fixed points are denoted by crimson, orange, purple, green, and yellow dots, respectively. The transition between each two of the three gapped $\mathrm{SO}(8)_i$ GN phases is through either the G_2 TCI phase or the Luttinger liquid (LL) critical phase. The triality relation is manifest in the D_3 symmetry of the phase diagram. In (b), the SO(8) GN, $\mathrm{SO}(7)_M$ GN, $\mathrm{SO}(8)_M$ GN, G_2 TCI, and free Majorana fixed points are denoted by brown, indigo, purple, green, and yellow dots, respectively. The transition between the SO(8) GN and the $\mathrm{SO}(8)_M$ GN phases is through the critical $\mathrm{SO}(7)_M$ GN phase in the Ising universality class. The embedding of the $u = v$ axis in the lattice model phase diagram is shown in red, whose positive and negative semi-axes are embedded in the G_2 TCI and the critical $\mathrm{SO}(7)_M$ GN phases, respectively.

A possible embedding of the u-axis is shown in figure 1. According to (3.3), in the parameter space of the continuum model (2.9), the u-axis of the lattice model (2.6) possessing the $\mathrm{SO}(7)_A$ symmetry is parameterized as

$$u\text{-axis}: \; t_A = \left(2 - \frac{k}{2}\right) g, \; t_B = kg, \; t_M = kg, \tag{4.1}$$

where k is a constant to be determined. Based on the triality mapping, the v-axis possessing the $\mathrm{SO}(7)_B$ symmetry is obtained by switching A and B and fixing M, hence, it is parameterized as

$$v\text{-axis}: \; t_A = kg, \; t_B = \left(2 - \frac{k}{2}\right) g, \; t_M = kg \tag{4.2}$$

Therefore, the phase diagram of the lattice model (2.6) spanned by u-axis and v-axis is given by

$$P_{\text{Lat}}: \; t_A + t_B = \left(2 + \frac{k}{2}\right) g, \; t_M = kg. \tag{4.3}$$

To determine the value of k, the $u = v$ axis is checked in the lattice model phase diagram. The lattice Hubbard type interaction (2.6) is invariant under the transformation $\chi_0(i) H_{\text{int}} \chi_0(i) = H_{\text{int}}$ [9]. Hence, χ_0 cannot appear in the local interaction of H_{int}. In other words, χ_0 decouples from other Majorana modes, and hence, the system should be gapless along the entire $u = v$ axis. In P_{Lat}, the $u = v$ axis reads

$$u = v: \; t_A = t_B = \left(1 + \frac{k}{4}\right) g, \; t_M = kg, \tag{4.4}$$

which lies in the fixed body $t_A = t_B$. To have both its positive and negative semi-axes embedded in gapless phases, the only choice of k is $k = -4$.

The reasoning why the $\text{SO}(7)_M$ is absent in the lattice Hamiltonian (2.6) is presented below. The equation of $\text{SO}(7)_M$ fixed plane P_M for the continuum Hamiltonian density is given by $t_A = t_B = 4g - 2t_M$. However, the u-v plane (4.3) of P_{Lat} with $k = -4$ substituted, i.e., $t_A + t_B = 0$ and $t_M = -4g$ is incompatible with the $\text{SO}(7)_M$ fixed plane P_M, except the trivial case of $g = t_A = t_B = t_M = 0$, i.e. $u = v = 0$. The triality among three SO(7) symmetries in the continuum model is broken to the duality of $\text{SO}(7)_A$ and $\text{SO}(7)_B$ on the lattice. This is a reminiscence of triality upon lattice regularization.

We need to figure out how the lattice Hamiltonian (2.6) with $u = v > 0$ and < 0 matches the G_2 critical TCI fixed point and $\text{SO}(7)_M$ critical ones, respectively. For the G_2 TCI fixed flow (3.9), the case of $u = v > 0$ of the lattice Hamiltonian should match the case $g > 0$ of the continuum one. Thus the positive semi-axis of $u = v$ should be embedded in the G_2 critical phase, and then naturally the negative semi-axis is embedded in the $\text{SO}(7)_M$ critical phase, as shown in figures 2 and 3(b). Consequently, in the lattice model interaction with $u = v > 0$ flows to the G_2 critical TCI fixed point, and that of $u = v < 0$ flows to the $\text{SO}(7)_M$ critical fixed point.

The phase diagram of the lattice model Hamiltonian (2.6) is shown in figure 4(a), supplemented by a numerical integration of the RG equations on the embedded lattice model phase diagram $P_{\text{Lat}}: \; t_A + t_B = 0, \; t_M = -4g$ (see appendix D for details). The Ising transition line between $\text{SO}(8)_A$ ($\text{SO}(8)_B$) GN phase and SO(8) GN phase is located at $u = -7v$ ($v = -7u$), which perfectly agrees with the mean-field analysis of the lattice model [9]. The embedding of the lattice phase diagram is shown in figure 4(b). The u-axis possesses the $\text{SO}(7)_A$ symmetry. Compared to the phase diagram of the continuum model shown in figure 1, the sign of g in the continuum Hamiltonian density follows that of u, while that of y is opposite to u. Hence, the positive u-axis is embedded in the $\text{SO}(8)_A$ GN phase, and its negative axis is embedded in the SO(8) GN phase. By the triality mapping, the positive v-axis is embedded in the $\text{SO}(8)_B$ GN phase, and the negative v-axis is also in the SO(8) GN phase.

For the $u = v$ axis, its negative semi-axis ($u = v < 0$) embedded in the critical $\text{SO}(7)_M$ GN phase is a branch cut lying inside the gapped SO(8) GN phase. Its gaplessness is due to the decoupled free Majorana χ_0, which is consistent with the analysis of the $u = v$ axis in the lattice model [9]. This criticality sandwiched in the same phase is an example of the unnecessary criticality [16, 17]. On the other hand, the positive $u = v$ semi-axis, embedded in the G_2 critical phase, describes the transition between $\text{SO}(8)_A$ GN and $\text{SO}(8)_B$ GN phases in the lattice model. Such a transition on lattice inherits the universality class and the central charge $c = \frac{7}{10} + \frac{1}{2}$ of the G_2 TCI phase in the continuum.

The spacetime supersymmetry in the G_2 TCI phase also has a reminiscence on the lattice. For a CFT with $\mathcal{N} = 1$ spacetime supersymmetry, the primary fields come in pairs. Within each pair the two primary fields have scaling dimension differed by $\frac{1}{2}$, and hence can be

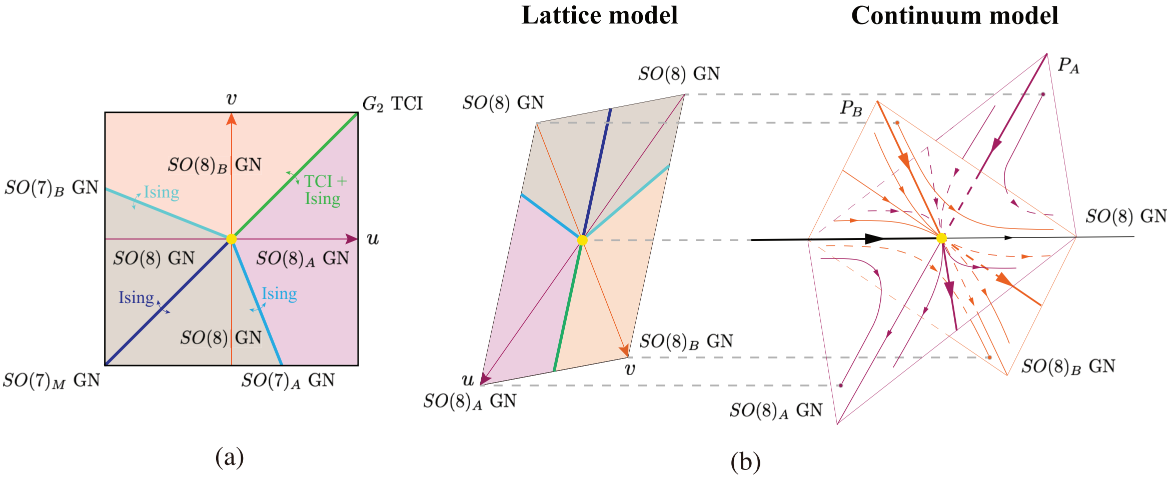

Figure 4. (a) The lattice model phase diagram. There are totally three gapped phases, belonging to SO$(8)_A$ GN, SO$(8)_B$ GN, and SO(8) GN phases in the continuum model. The phase transition between SO$(8)_A$ GN and SO$(8)_B$ GN phases, marked as the green segment, is located at $u = v > 0$, and described by G_2 TCI phase in the continuum model. The phase transition between SO$(8)_A$ (SO$(8)_B$) GN and SO(8) GN phases, represented by the blue (turquoise) segment, is located at $u = -7v$ ($v = -7u$) and belongs to the critical SO$(7)_A$ (SO$(7)_B$) GN phase in the continuum model. Inside the SO(8) GN phase there is a branch cut colored in indigo, on which the system becomes gapless. It is located at $u = v < 0$ and described by the critical SO$(7)_M$ GN phase in the continuum model. (b) Embedding of the lattice model phase diagram into the continuum model phase diagram. RG flows of the continuum model in body $4g - 2t_A - 2t_B + t_M = 0$ (not a fixed body) spanned by SO$(7)_A$ and SO$(7)_B$ symmetric fixed planes (P_A and P_B) are shown in the right. On each SO(7) symmetric fixed plane the RG flows are the same as figure 2(a) ensured by the triality. The phase boundaries are marked as thick segments. P_A and P_B, as well as RG flows on them, are colored in crimson and orange, respectively. The lattice model phase diagram is shown in the left part. The u/v-axis is embedded in $P_{A/B}$ as a straight line.

viewed as the supersymmetry partner of each other. For example, for the TCI CFT described by (3.9), the stress-energy tensor for right-mover $T^R_B \sim C_{abcd}\chi^R_{a+1}\chi^R_{b+1}\chi^R_{c+1}\chi^R_{d+1}$ with scaling dimension 2 has a supersymmetry partner $T^R_F \sim C_{abc}\chi^R_{a+1}\chi^R_{b+1}\chi^R_{c+1}$ with scaling dimension $\frac{3}{2}$ [13] (this operator is also called ϵ'' in CFT literature). Typically, a lattice model with low energy effective theory governed by a supersymmetric CFT exhibits quantum mechanical supersymmetry [33, 34]. Similar to the supersymmetric CFT, in a lattice model with $\mathcal{N} = 1$ quantum mechanical supersymmetry, the eigenstates of the Hamiltonian H_{SUSY} also come in pairs, within which the two states have different fermion parity and related to each other by a supercharge operator Q satisfying $H_{\text{SUSY}} = Q^2$. This phenomenon particularly resembles the G_2 invariant lattice model (2.6) when $u = v$, which exhibits the degeneracy between bosonic and fermionic states on each site [9]. The "supercharge operator" switching bosonic and fermionic states on site i is just the Majorana operator $\chi_0(i)$. However, this is not an authentic supersymmetry since $H^{G_2}_{\text{int}} \neq (\sum_i \chi_0(i))^2$, and hence does not satisfy the definition of the quantum mechanical supersymmetry. Nevertheless, this degeneracy between on-site bosonic and fermionic states can still be viewed as the lattice reminiscence of the spacetime supersymmetry in the continuum model.

Before closure, we briefly comment the fate of spacetime supersymmetry at $u = v$ in higher dimensions. In spatial dimension $d > 1$, sufficiently strong u and v will drive G_2 symmetry to be spontaneously broken to SU(3) or SU(2) × U(1) [9], with order parameters transformed in the 7-dimensional vector representation or both 7-dimensional vector and 14-dimensional adjoint representations, respectively. Upon Hubbard-Stratonovich transformation, scalar boson fields are introduced and coupled to the Majorana fermions through a Yukawa-type interaction. We first consider the case of $u = v < 0$, where totally 21 scalar boson fields are introduced in the Hubbard-Stratonovich transformation to capture the spontaneous breaking of G_2 to SU(2) × U(1). 7 of the bosons are transformed in the 7-vector representation of G_2, while the other 14 are in the adjoint representation. The adjoint bosons do not have fermionic partners, and hence spacetime supersymmetry is not expected.

For $u = v > 0$, 7 bosons are introduced transformed as the 7-vector of G_2. When $u < u_c$, these bosons are gapped, corresponding to the G_2 symmetric phase where all the 8 Majoranas are gapless. When $u > u_c$, condensation of the bosons spontaneously breaks G_2 down to SU(3). Consequently, 6 out of 8 Majoranas are gapped, composing a 3-component complex fermion transformed in the 3-spinor representation of SU(3) [9]. The rest 2 gapless Majoranas always include χ_0 which remains decoupled and gapless on the entire $u = v$ line. At the critical point $u = u_c$, all bosons and Majoranas become gapless simultaneously, while 7 Majoranas χ_m, $1 \leq m \leq 7$, are transformed in the same 7-vector representation of G_2 as the 7 real bosons, signaling a plausible supersymmetry structure. A necessary condition for an authentic spacetime supersymmetry is that the low energy Majoranas must be relativistic in order to be supersymmetry partners of the scalar bosons, which can be realized in topological superconductors [35–37]. In this case, upon Hubbard-Stratonovich transformation, the critical theory for $u = u_c$ is a Gross-Neveu-Yukawa theory [24] with 7-flavor scalar bosons and Majorana fermions (decoupled χ_0 omitted):

$$\mathcal{L} = \bar{\chi}_m (i\gamma^\mu \partial_\mu \delta_{mn} - i\tilde{C}_{mnp}\varphi_p)\chi_n + U(\varphi). \tag{4.5}$$

Here γ^μ are gamma matrices, $\tilde{C}_{mnp} = C_{(m-1)(n-1)(p-1)}$, and $U(\varphi)$ is the quartic self-interaction of the scalar boson φ_m. Details of the Hubbard-Stratonovich transformation is given in appendix A. Spacetime supersymmetry requires the existence of superpotential W satisfying [38]

$$\frac{1}{2}\frac{\partial^2 W}{\partial\varphi_m \partial\varphi_n} = i\tilde{C}_{mnp}\varphi_p, \qquad \left(\frac{\partial W}{\partial \varphi_m}\right)^2 = U(\varphi). \tag{4.6}$$

However, the former equality is self-conflicting since $\tilde{C}_{mnp}$ is fully anti-symmetric. Therefore, we conclude that supersymmetry cannot emerge at $u = v$ of the lattice model (2.6) in higher dimensions.

5 Conclusions

In summary, we investigate the low energy effective theory of the minimal G_2 symmetric lattice model [9] in (1+1)D by an one-loop RG method. The SO(8) triality, which is absent in the lattice model due to the on-site Hubbard-type interactions, emerges naturally in the low energy effective theory as a triality mapping among three different SO(7) symmetries, and consequently three gapped phases as well as three Ising critical phases. The phase transitions between phases related by the triality relation are unified by either a Luttinger liquid phase, or a G_2 symmetric multi-critical phase. This G_2 multi-critical phase is described by a direct product of Ising and TCI CFTs with central charge $c = \frac{1}{2} + \frac{7}{10} = \frac{6}{5}$, and possesses emergent spacetime supersymmetry carried by the TCI CFT. When the continuum model is regularized on a lattice, the triality among three SO(7) symmetries is broken to the duality of two SO(7) symmetries [9], eliminating the third one. The spacetime supersymmetry is also degraded to a degeneracy pattern between the on-site bosonic and fermionic states, instead of an authentic quantum mechanical supersymmetry. However, these reminiscences in ultraviolet still imply clues of exotic structures in infrared, as explored in the current work.

Acknowledgments

ZQG acknowledges D.-H. Lee, H. Yang, Y.-Q. Wang, Z. Han, and J.-C. Feng for helpful discussions. CW is supported by the National Natural Science Foundation of China under the Grant No. 12234016 and No. 12174317. This work has been supported by the New Cornerstone Science Foundation.

A Fermion bilinears and majorana operators in the lattice model

Define four by four gamma matrices as

$$\Gamma^1 = \begin{pmatrix} 0 & -iI \\ iI & 0 \end{pmatrix}, \quad \Gamma^{2,3,4} = \begin{pmatrix} \vec{\sigma} & 0 \\ 0 & -\vec{\sigma} \end{pmatrix}, \quad \Gamma^5 = \begin{pmatrix} 0 & I \\ I & 0 \end{pmatrix}, \tag{A.1}$$

where I and $\vec{\sigma}$ are two by two identity and Pauli matrices. These five gamma matrices form an Sp(4) vector. The generators of Sp(4) are defined as $\Gamma^{ab} = -\frac{i}{2}[\Gamma^a, \Gamma^b]$, and the charge conjugation operator is defined as $R = \Gamma^1\Gamma^3$. Therefore, the femion bilinears on each site i, $N_{ab}(i)$ with $0 \le a, b \le 7$, spanning an SO(8) algebra reads

$$N_{ab}(i) = -\frac{1}{2}\psi^\dagger(i)\Gamma^{ab}\psi(i), \qquad 1 \le a, b \le 5, \tag{A.2}$$

$$N_{a7}(i) = \frac{1}{2}\psi^\dagger(i)\Gamma^{a}\psi(i), \qquad 1 \le a \le 5, \tag{A.3}$$

$$N_{06}(i) = \frac{1}{2}\psi^\dagger(i)\psi(i) - 1, \tag{A.4}$$

$$N_{0a}(i) + iN_{a6}(i) = -\frac{i}{2}\mathrm{sgn}(i)\psi^\dagger(i)\Gamma^a R\psi^\dagger(i), \quad 1 \le a \le 5, \tag{A.5}$$

$$N_{07}(i) - iN_{67}(i) = \frac{1}{2}\mathrm{sgn}(i)\psi^\dagger(i)R\psi^\dagger(i), \tag{A.6}$$

where $\mathrm{sgn}(i) = \pm 1$ is staggered on two sublattices of the bipartite lattice. The Majorana operators, transformed under the vector representation of SO(8), are defined as

$$\chi_1(i) = e^{-i\mathrm{sgn}(i)\pi/4}\psi_{\frac{1}{2}}(i) + e^{i\mathrm{sgn}(i)\pi/4}\psi^\dagger_{\frac{1}{2}}(i),$$
$$\chi_2(i) = -e^{i\mathrm{sgn}(i)\pi/4}\psi_{\frac{1}{2}}(i) - e^{-i\mathrm{sgn}(i)\pi/4}\psi^\dagger_{\frac{1}{2}}(i),$$

Weight μ	Bosonic vector	Fermionic vector	Majorana vector
$(\frac{\sqrt{3}}{2},\frac{1}{2})$	$\psi^\dagger_{\frac{1}{2}}\psi^\dagger_{-\frac{3}{2}}\|0\rangle$	$\psi^\dagger_{\frac{3}{2}}\psi^\dagger_{\frac{1}{2}}\psi^\dagger_{-\frac{3}{2}}\|0\rangle$	$\frac{1}{2}(\chi_1+i\chi_2)$
$(0,1)$	$\psi^\dagger_{\frac{3}{2}}\psi^\dagger_{\frac{1}{2}}\psi^\dagger_{-\frac{1}{2}}\psi^\dagger_{-\frac{3}{2}}\|0\rangle$	$\psi^\dagger_{\frac{1}{2}}\psi^\dagger_{-\frac{1}{2}}\psi^\dagger_{-\frac{3}{2}}\|0\rangle$	$\frac{1}{2}(\chi_6-i\chi_7)$
$(-\frac{\sqrt{3}}{2},\frac{1}{2})$	$\psi^\dagger_{-\frac{1}{2}}\psi^\dagger_{-\frac{3}{2}}\|0\rangle$	$\psi^\dagger_{\frac{3}{2}}\psi^\dagger_{-\frac{1}{2}}\psi^\dagger_{-\frac{3}{2}}\|0\rangle$	$\frac{1}{2}(\chi_3-i\chi_5)$
$(-\frac{\sqrt{3}}{2},-\frac{1}{2})$	$\psi^\dagger_{\frac{3}{2}}\psi^\dagger_{-\frac{1}{2}}\|0\rangle$	$\psi^\dagger_{-\frac{1}{2}}\|0\rangle$	$\frac{1}{2}(\chi_1-i\chi_2)$
$(0,-1)$	$\|0\rangle$	$\psi^\dagger_{\frac{3}{2}}\|0\rangle$	$\frac{1}{2}(\chi_6+i\chi_7)$
$(\frac{\sqrt{3}}{2},-\frac{1}{2})$	$\psi^\dagger_{\frac{3}{2}}\psi^\dagger_{\frac{1}{2}}\|0\rangle$	$\psi^\dagger_{\frac{1}{2}}\|0\rangle$	$\frac{1}{2}(\chi_3+i\chi_5)$
$(0,0)$	$\frac{1}{\sqrt{2}}(\psi^\dagger_{\frac{3}{2}}\psi^\dagger_{-\frac{3}{2}}+\psi^\dagger_{\frac{1}{2}}\psi^\dagger_{-\frac{1}{2}})\|0\rangle$	$\frac{1}{\sqrt{2}}(\psi^\dagger_{-\frac{3}{2}}\pm i\psi^\dagger_{\frac{3}{2}}\psi^\dagger_{\frac{1}{2}}\psi^\dagger_{-\frac{1}{2}})\|0\rangle$	χ_4
Weight μ	**Bosonic singlet**	**Fermionic singlet**	**Majorana singlet**
(0,0)	$\frac{1}{\sqrt{2}}(\psi^\dagger_{\frac{3}{2}}\psi^\dagger_{-\frac{3}{2}}-\psi^\dagger_{\frac{1}{2}}\psi^\dagger_{-\frac{1}{2}})\|0\rangle$	$\frac{1}{\sqrt{2}}(\psi^\dagger_{-\frac{3}{2}}\mp i\psi^\dagger_{\frac{3}{2}}\psi^\dagger_{\frac{1}{2}}\psi^\dagger_{-\frac{1}{2}})\|0\rangle$	χ_0

Table 2. Bosonic states, fermionic states, and Majorana operators classified by G_2 weight. The $\pm$ signs in the $(0,0)$ weight states are staggered on sublattices. The site label is omitted for clarity.

$$\begin{aligned}\chi_3(i) &= e^{-i\text{sgn}(i)\pi/4}\psi_{-\frac{1}{2}}(i)+e^{i\text{sgn}(i)\pi/4}\psi^\dagger_{-\frac{1}{2}}(i),\\ \chi_4(i) &= -e^{i\text{sgn}(i)\pi/4}\psi_{\frac{3}{2}}(i)-e^{-i\text{sgn}(i)\pi/4}\psi^\dagger_{\frac{3}{2}}(i),\\ \chi_5(i) &= e^{i\text{sgn}(i)\pi/4}\psi_{-\frac{1}{2}}(i)+e^{-i\text{sgn}(i)\pi/4}\psi^\dagger_{-\frac{1}{2}}(i),\\ \chi_6(i) &= e^{-i\text{sgn}(i)\pi/4}\psi_{-\frac{3}{2}}(i)+e^{i\text{sgn}(i)\pi/4}\psi^\dagger_{-\frac{3}{2}}(i),\\ \chi_7(i) &= e^{i\text{sgn}(i)\pi/4}\psi_{-\frac{3}{2}}(i)+e^{-i\text{sgn}(i)\pi/4}\psi^\dagger_{-\frac{3}{2}}(i)\\ \chi_0(i) &= e^{-i\text{sgn}(i)\pi/4}\psi_{\frac{3}{2}}(i)+e^{i\text{sgn}(i)\pi/4}\psi^\dagger_{\frac{3}{2}}(i),\end{aligned} \tag{A.7}$$

where $\chi_{1,2,\ldots,7}(i)$ form a G_2 vector while $\chi_0(i)$ is a G_2 singlet. In fact, $\chi_{1,2,\ldots,7}(i)$ also form a vector of $\text{SO}(7)_M$ spanned by $i\chi_m(i)\chi_n(i)$ with $1\le m,n\le 7$, which is absent in the lattice model. The G_2 weights of these Majorana fermions are given in table 2. As a comparison, the weight of bosonic and fermionic states are also listed.

In this Majorana basis, the lattice Hamiltonian reads (constant term neglected)

$$\begin{aligned}H_0 &= \frac{it_{\text{hop}}}{2}\Big(\sum_i \chi_0(i)\chi_0(i+1)+\chi_1(i)\chi_1(i+1)+\chi_3(i)\chi_3(i+1)+\chi_6(i)\chi_6(i+1)\\ &\qquad -\chi_2(i)\chi_2(i+1)-\chi_4(i)\chi_4(i+1)-\chi_5(i)\chi_5(i+1)-\chi_7(i)\chi_7(i+1)\Big)+h.c.\end{aligned} \tag{A.8}$$

$$\begin{aligned}H^{G_2}_{\text{int}} &= -\frac{u+v}{32}\sum_i C_{abcd}\chi_{a+1}(i)\chi_{b+1}(i)\chi_{c+1}(i)\chi_{d+1}(i)\\ &\quad+\frac{u-v}{8}\sum_i \chi_0(i)C_{abc}\chi_{a+1}(i)\chi_{b+1}(i)\chi_{c+1}(i),\end{aligned} \tag{A.9}$$

where the structure constant of octonions C_{abc} is chosen as $C_{031}=C_{052}=C_{064}=C_{126}=C_{154}=C_{243}=C_{365}=1$ with dual tensor $C_{ijkl}=\frac{1}{6}\epsilon_{ijklabc}C_{abc}$. When $u=v$, the interaction

Hamiltonian reads

$$H_{\text{int}}^{G_2} = \frac{3}{2}u\sum_i G_{ab}(i)^2 = -\frac{u}{16}\sum_i C_{abcd}\chi_{a+1}(i)\chi_{b+1}(i)\chi_{c+1}(i)\chi_{d+1}(i), \tag{A.10}$$

from which it can be seen that only 7 out of 8 Majoranas, except for $\chi_0(i)$, appear in this Hamiltonian. It can be rearranged as

$$H_{\text{int}}^{G_2} = -\frac{u}{16}\sum_i \left(iC_{mab}\chi_{a+1}(i)\chi_{b+1}(i)\right)\left(iC_{mcd}\chi_{c+1}(i)\chi_{d+1}(i)\right), \tag{A.11}$$

where identity $C_{mab}C_{mcd} = -C_{abcd}+\delta_{ac}\delta_{bd}-\delta_{ad}\delta_{bc}$ is used. Therefore, a Hubbard-Stratonovich transformation generates a Yukawa coupling between Majorana χ_a and scalar boson ϕ_a as $iC_{abc}\chi_{a+1}\chi_{b+1}\phi_{c+1}$.

B RG equations

The current algebras read (constant terms neglected since they do not contribute to the RG equations)

$$\begin{aligned}
G_{ab}^R(z)G_{cd}^R(w) \sim{}& \frac{1}{z-w}\Big(\frac{2}{3}\delta_{ac}G_{bd}^R(w)+\frac{2}{3}\delta_{bd}G_{ac}^R(w)-\frac{2}{3}\delta_{ad}G_{bc}^R(w)-\frac{2}{3}\delta_{ac}G_{bd}^R(w) \\
&+\frac{1}{6}C_{bcam}G_{md}^R(w)+\frac{1}{6}C_{dabm}G_{mc}^R(w)-\frac{1}{6}C_{bcdm}G_{ma}^R(w)-\frac{1}{6}C_{dacm}G_{mb}^R(w)\Big)
\end{aligned} \tag{B.1}$$

$$G_{ab}^R(z)T_c^R(w) \sim \frac{1}{z-w}\left(\frac{2}{3}\delta_{bc}T_a^R(w)-\frac{2}{3}\delta_{ac}T_b^R(w)+\frac{1}{3}C_{abcd}T_d^R(w)\right), \tag{B.2}$$

$$G_{ab}^R(z)V_c^R(w) \sim \frac{1}{z-w}\left(\frac{2}{3}\delta_{bc}V_a^R(w)-\frac{2}{3}\delta_{ac}V_b^R(w)+\frac{1}{3}C_{abcd}V_d^R(w)\right), \tag{B.3}$$

$$T_a^R(z)T_b^R(w) \sim \frac{1}{z-w}\left(-G_{ab}^R(w)+\frac{1}{\sqrt{3}}C_{abc}T_c^R(w)\right), \tag{B.4}$$

$$T_a^R(z)V_b^R(w) \sim \frac{1}{z-w}\left(-\frac{1}{\sqrt{3}}C_{abc}V_c^R(w)\right), \tag{B.5}$$

$$V_a^R(z)V_b^R(w) \sim \frac{1}{z-w}\left(-G_{ab}^R(w)-\frac{1}{\sqrt{3}}C_{abc}T_c^R(w)\right), \tag{B.6}$$

and for left-handed currents the current algebra is the same, except for z substituted by $\bar{z}$. The WZW level is irrelevant to the one-loop RG of interaction Hamiltonian density, so it is simply dropped. Consider operator product expansions (OPE) showing up in the calculation of one-loop RG as follows.

1.

$$G_{ab}^R(z)G_{ab}^L(\bar{z})G_{cd}^R(w)G_{cd}^L(\bar{w}) \sim \frac{1}{|z-w|^2}\frac{4}{9}\left(\delta\cdot G^R+\frac{1}{4}C\cdot G^R\right)\left(\delta\cdot G^L+\frac{1}{4}C\cdot G^L\right), \tag{B.7}$$

where shorthands $\delta\cdot G$ and $C\cdot G$ are used to represent four δ-terms and four C-terms in (B.1) for simplicity. Consider $(\delta\cdot G^R)(\delta\cdot G^L)$ first.

$$\begin{aligned}(\delta\cdot G^R)(\delta\cdot G^L) &= (\delta_{ac}G^R_{bd}+\delta_{bd}G^R_{ac}-\delta_{ad}G^R_{bc}-\delta_{ac}G^R_{bd})(\delta_{ac}G^L_{bd}+\delta_{bd}G^L_{ac}-\delta_{ad}G^L_{bc}-\delta_{ac}G^L_{bd})\\ &= -2\delta_{ad}\delta_{ac}G^R_{bc}G^L_{bd}-2\delta_{ad}\delta_{bd}G^R_{bc}G^L_{ac}-2\delta_{bc}\delta_{ac}G^R_{ad}G^L_{bd}-2\delta_{bc}\delta_{bd}G^R_{ad}G^L_{ac}\\ &\quad -2\delta_{bc}\delta_{ac}G^R_{ad}G^L_{bd}+2\delta_{ad}\delta_{bc}G^R_{bc}G^L_{ad}+2\delta_{ac}\delta_{bd}G^R_{ac}G^L_{bd}+4\delta_{cd}\delta_{cd}G^R_{ab}G^L_{ab}\\ &= -2\times 4G^R_{ab}G^L_{ab}+0+4\times 7G^R_{ab}G^L_{ab}\\ &= 20G^R_{ab}G^L_{ab}, \end{aligned} \tag{B.8}$$

where identities $G_{ab}=-G_{ba}$, $\delta_{ab}G_{ab}=0$ and $\delta_{ab}\delta_{ab}=7$ are employed in passsing to the third equality. Then consider $(C\cdot G^R)(C\cdot G^L)$.

$$\begin{aligned}(C\cdot G^R)(C\cdot G^L) &= 4C_{dacm}G^R_{mb}C_{dacn}G^L_{nb}+4C_{dacm}G^R_{mb}C_{dabn}G^L_{nc}\\ &= 4\times 24\delta_{mn}G^R_{mb}G^L_{nb}+4\times\left(-2C_{cmbn}+4(\delta_{cb}\delta_{mn}-\delta_{cn}\delta_{bm})\right)G^R_{mb}G^L_{nc}\\ &= 96G^R_{ab}G^L_{ab}+8C_{abcd}G^R_{ab}G^L_{cd}+4G^R_{ab}G^L_{ab}-4\times 0\\ &= 96G^R_{ab}G^L_{ab}+16G^R_{ab}G^L_{ab}+16G^R_{ab}G^L_{ab}\\ &= 128G^R_{ab}G^L_{ab}, \end{aligned} \tag{B.9}$$

where identities $C_{mnab}C_{mncd}=-2C_{abcd}+4(\delta_{ac}\delta_{bd}-\delta_{ad}\delta_{bc})$ and $C_{abcm}C_{abcn}=24\delta_{mn}$ are employed in the second equality, and identities $C_{abcd}G_{cd}=2G_{ab}$ and $G_{ab}=-G_{ba}$ are employed in the fourth equality. Then consider $(\delta\cdot G^R)(C\cdot G^L)+(C\cdot G^R)(\delta\cdot G^L)$.

$$\begin{aligned}(\delta\cdot G^R)(C\cdot G^L)+(C\cdot G^R)(\delta\cdot G^L) &= 4C_{dacm}G^R_{mc}G^L_{ad}+4C_{bcam}G^R_{mb}G^L_{ac}\\ &\quad -4C_{dacm}G^R_{ma}G^L_{cd}-4C_{bcam}G^R_{bc}G^L_{ma}\\ &= 4\times 4C_{abcd}G^R_{ab}G^L_{cd}\\ &= 32G^R_{ab}G^L_{ab}, \end{aligned} \tag{B.10}$$

where identities $\delta_{ab}C_{abcd}=0$ and $C_{abcd}G_{cd}=2G_{ab}$ are employed. In summary, the OPE of $G^R_{ab}(z)G^L_{ab}(\bar z)G^R_{cd}(w)G^L_{cd}(\bar w)$ gives rise to

$$\begin{aligned}G^R_{ab}(z)G^L_{ab}(\bar z)G^R_{cd}(w)G^L_{cd}(\bar w) &\sim \frac{1}{|z-w|^2}\frac{4}{9}\left(20+\frac{1}{16}\times 128+\frac{1}{4}\times 32\right)G^R_{ab}G^L_{ab}\\ &= \frac{1}{|z-w|^2}16G^R_{ab}G^L_{ab}. \end{aligned} \tag{B.11}$$

2.

$$\begin{aligned}T^R_a(z)T^L_a(\bar z)T^R_b(w)T^L_b(\bar w) &\sim \frac{1}{|z-w|^2}\left(-G^R_{ab}+\frac{1}{\sqrt3}C_{abc}T^R_c\right)\left(-G^L_{ab}+\frac{1}{\sqrt3}C_{abd}T^L_d\right)\\ &= \frac{1}{|z-w|^2}\left(G^R_{ab}G^L_{ab}+2T^R_aT^L_a\right), \end{aligned} \tag{B.12}$$

where identities $C_{abc}G_{bc}=0$ and $C_{abc}C_{abd}=6\delta_{cd}$ are employed.

3.

$$
\begin{aligned}
V_a^R(z)V_a^L(\bar z)V_b^R(w)V_b^L(\bar w) &\sim \frac{1}{|z-w|^2}\left(-G_{ab}^R-\frac{1}{\sqrt{3}}C_{abc}T_c^R\right)\left(-G_{ab}^L-\frac{1}{\sqrt{3}}C_{abd}T_d^L\right)\\
&=\frac{1}{|z-w|^2}\left(G_{ab}^RG_{ab}^L+2T_a^RT_a^L\right), \qquad \text{(B.13)}
\end{aligned}
$$

where identities $C_{abc}G_{bc}=0$ and $C_{abc}C_{abd}=6\delta_{cd}$ are employed.

4.

$$
\begin{aligned}
G_{ab}^R(z)G_{ab}^L(\bar z)T_c^R(w)T_c^L(\bar w) \;&\sim\; \frac{1}{|z-w|^2}\left(\frac{2}{3}\delta_{bc}T_a^R-\frac{2}{3}\delta_{ac}T_b^R+\frac{1}{3}C_{abcd}T_d^R\right)\\
&\qquad\times\left(\frac{2}{3}\delta_{bc}T_a^L-\frac{2}{3}\delta_{ac}T_b^L+\frac{1}{3}C_{abce}T_e^L\right)\\
&=\frac{1}{|z-w|^2}\left(\frac{4}{9}(\delta_{bc}T_a^R-\delta_{ac}T_b^R)(\delta_{bc}T_a^L-\delta_{ac}T_b^L)\right.\\
&\qquad\left.+\frac{1}{9}C_{abcd}C_{abce}T_d^RT_e^L\right)\\
&=\frac{1}{|z-w|^2}\frac{1}{9}(4\times 2\times 7T_a^RT_a^L-4\times 2T_a^RT_a^L+24\delta_{de}T_d^RT_e^L)\\
&=\frac{1}{|z-w|^2}8T_a^RT_a^L, \qquad \text{(B.14)}
\end{aligned}
$$

where identities $\delta_{ab}\delta_{ab}=7$, $\delta_{ab}C_{abcd}=0$ and $C_{abcm}C_{abcn}=24\delta_{mn}$ are employed. Since both T_a and V_a forms G_2 vector representations, the result above can be directly generalized to the OPE below:

$$
G_{ab}^R(z)G_{ab}^L(\bar z)V_c^R(w)V_c^L(\bar w)\sim\frac{1}{|z-w|^2}8V_a^RV_a^L, \qquad \text{(B.15)}
$$

$$
G_{ab}^R(z)G_{ab}^L(\bar z)\left(V_c^R(w)T_c^L(\bar w)+T_c^R(w)V_c^L(\bar w)\right)\sim\frac{1}{|z-w|^2}8\left(V_a^RT_a^L+T_a^RV_a^L\right). \qquad \text{(B.16)}
$$

5.

$$
\begin{aligned}
T_a^R(z)T_a^L(\bar z)V_b^R(w)V_b^L(\bar w) &\sim \frac{1}{|z-w|^2}\frac{1}{3}C_{abc}C_{abd}V_c^RV_d^L\\
&=\frac{1}{|z-w|^2}\frac{1}{3}\times 6\delta_{cd}V_c^RV_d^L\\
&=\frac{1}{|z-w|^2}2V_a^RV_a^L. \qquad \text{(B.17)}
\end{aligned}
$$

6.

$$
\begin{aligned}
&\left(V_a^R(z)T_a^L(\bar z)+T_a^R(z)V_a^L(\bar z)\right)\left(V_b^R(w)T_b^L(\bar w)+T_b^R(w)V_b^L(\bar w)\right)\\
&\sim\frac{1}{|z-w|^2}2\left(\left(-G_{ab}^R+\frac{1}{\sqrt{3}}C_{abc}T_c^R\right)\left(-G_{ab}^L-\frac{1}{\sqrt{3}}C_{abd}T_d^L\right)\right.\\
&\quad\left.+\,2\left(-\frac{1}{\sqrt{3}}C_{abc}V_c^R\right)\left(-\frac{1}{\sqrt{3}}C_{abd}V_d^L\right)\right)\\
&=\frac{1}{|z-w|^2}\left(2G_{ab}^RG_{ab}^L-4T_a^RT_a^L+4V_a^RV_a^L\right), \qquad \text{(B.18)}
\end{aligned}
$$

where identities $C_{abc}G_{bc}=0$ and $C_{abc}C_{abd}=6\delta_{cd}$ are employed.

JHEP02(2025)202

7.

$$\begin{aligned}
&T_a^R(z)T_a^L(\bar{z})\left(V_b^R(w)T_b^L(\bar{w})+T_b^R(w)V_b^L(\bar{w})\right)\\
&\sim\frac{1}{|z-w|^2}\left(\left(-G_{ab}^R+\frac{1}{\sqrt{3}}C_{abc}T_c^R\right)\left(-\frac{1}{\sqrt{3}}C_{abd}V_d^L\right)\right.\\
&\quad\left.+\left(-\frac{1}{\sqrt{3}}C_{abc}V_c^R\right)\left(-G_{ab}^L-\frac{1}{\sqrt{3}}C_{abd}T_d^L\right)\right)\\
&=\frac{1}{|z-w|^2}\left(-2\left(V_a^RT_a^L+T_a^RV_a^L\right)\right),
\end{aligned} \tag{B.19}$$

where identities $C_{abc}G_{bc}=0$ and $C_{abc}C_{abd}=6\delta_{cd}$ are employed.

8.

$$\begin{aligned}
&V_a^R(z)V_a^L(\bar{z})\left(V_b^R(w)T_b^L(\bar{w})+T_b^R(w)V_b^L(\bar{w})\right)\\
&\sim\frac{1}{|z-w|^2}\left(\left(-G_{ab}^R-\frac{1}{\sqrt{3}}C_{abc}T_c^R\right)\left(-\frac{1}{\sqrt{3}}C_{abd}V_d^L\right)\right.\\
&\quad\left.-\left(-\frac{1}{\sqrt{3}}C_{abc}V_c^R\right)\left(-G_{ab}^L-\frac{1}{\sqrt{3}}C_{abd}T_d^L\right)\right)\\
&=\frac{1}{|z-w|^2}2\left(V_a^RT_a^L+T_a^RV_a^L\right),
\end{aligned} \tag{B.20}$$

where identities $C_{abc}G_{bc}=0$ and $C_{abc}C_{abd}=6\delta_{cd}$ are employed.

Combine the results of OPE $1\sim 8$. The OPE of interaction Hamiltonian density reads

$$\begin{aligned}
&\mathcal{H}_{\text{int}}(z,\bar{z})\mathcal{H}_{\text{int}}(w,\bar{w})\\
&\sim\frac{1}{|z-w|^2}\Big((16g^2+t^2+y^2+w^2)\sum_{a,b}G_{ab}^RG_{ab}^L+(16gt+2t^2+2y^2-2w^2)\sum_a T_a^RT_a^L\\
&\quad+(16gy+4ty+2w^2)\sum_a V_a^RV_a^L+(16gw-4tw+4yw)\frac{1}{\sqrt{2}}\sum_a\left(T_a^RV_a^L+V_a^RT_a^L\right)\Big),
\end{aligned} \tag{B.21}$$

which gives rise to the RG equations:

$$\begin{aligned}
\frac{\mathrm{d}g}{\mathrm{d}l}&=16g^2+t^2+y^2+w^2,\\
\frac{\mathrm{d}t}{\mathrm{d}l}&=16gt+2t^2+2y^2-2w^2,\\
\frac{\mathrm{d}y}{\mathrm{d}l}&=16gy+4ty+2w^2,\\
\frac{\mathrm{d}w}{\mathrm{d}l}&=16gw-4tw+4yw.
\end{aligned} \tag{B.22}$$

The RG equations can be solved analytically on SO(7) symmetric fixed planes. On the $\mathrm{SO}(7)_A$ symmetric fixed plane, namely $t=2g, w=0$, the RG equation have only two independent variables, which can be chosen as y and $x=g+\frac{t}{2}$. The RG equations are reduced to

$$\frac{\mathrm{d}y}{\mathrm{d}x}=\frac{6xy}{5x^2+y^2}, \tag{B.23}$$

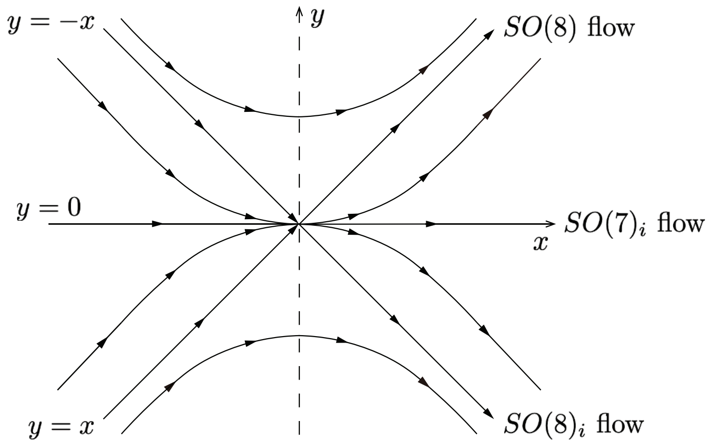

Figure 5. RG flow on SO(7) symmetric fixed planes.

whose solution is $(x^2-y^2)^3+Cy^5=0$, $\forall C\in\mathbb{R}$. This set of curves have asymptotic lines $y=x$, $y=-x$ and $y=0$, corresponding to the SO(8) GN fixed flow $t=y=2g, w=0$, the $\mathrm{SO}(8)_A$ GN fixed flow $t=-y=2g, w=0$, and the $\mathrm{SO}(7)_A$ GN fixed flow $t=2g, y=w=0$, respectively. The plot of these solution curves are shown in figure 5, which looks the same as figure 2 in the main text. According to the triality, the RG flows on the other two SO(7) symmetric fixed planes are the same.

The RG equations can be also investigated in terms of g, t_A, t_B, t_M by employing the relation between T'_a, V'_a, T''_a, V''_a and T_a, V_a. The OPE reads

$$\begin{aligned}&\mathcal{H}_{\text{int}}(z,\bar{z})\mathcal{H}_{\text{int}}(w,\bar{w})\\&\sim\frac{1}{|z-w|^2}\Bigg(\Big(16g^2+t_A^2+t_B^2+t_M^2+\frac{1}{2}t_At_B+\frac{1}{2}t_Bt_M+\frac{1}{2}t_Mt_A\Big)\sum_{a,b}G^R_{ab}G^L_{ab}\\&\qquad+\Big(16gt_A+2t_A^2+4t_Bt_M\Big)\sum_a T^R_aT^L_a+\Big(16gt_B+2t_B^2+4t_Mt_A\Big)\sum_a T'^R_aT'^L_a\\&\qquad+\Big(16gt_M+2t_M^2+4t_At_B\Big)\sum_a T''^R_aT''^L_a\Bigg),\end{aligned}\tag{B.24}$$

which gives rise to the RG equations in the main text:

$$\begin{aligned}\frac{\mathrm{d}g}{\mathrm{d}l}&=16g^2+\sum_i t_i^2+\frac{1}{4}\sum_{i\neq j}t_it_j,\\\frac{\mathrm{d}t_i}{\mathrm{d}l}&=16gt_i+2t_i^2+4\frac{t_At_Bt_M}{t_i},\end{aligned}\tag{B.25}$$

where i,j,k range in A,B,M. The RG flows on SO(7) fixed planes are the same as figure 5.

Except for fixed flows and fixed planes, the RG equations (B.25) also have fixed bodies, i.e. three dimensional bodies in the parameter space in which RG flows keep inside evolution.

From (B.25), it is not hard to derive that

$$\frac{\mathrm{d}}{\mathrm{d}l}\Big(\sum_i t_i\Big) = 16g\Big(\sum_i t_i\Big) + 2\Big(\sum_i t_i\Big)^2 \tag{B.26}$$

$$\frac{\mathrm{d}}{\mathrm{d}l}(t_i - t_j) = \Big(16g + 2t_i + 2t_j - 4\sum_k \epsilon_{ijk} t_k\Big)(t_i - t_j). \tag{B.27}$$

Therefore, both $\sum_i t_i = 0$ and $t_i = t_j$ are solutions to the RG equations (B.25), and hence define four fixed bodies in the parameter space: $t_A + t_B + t_M = 0$, $t_A = t_B$, $t_B = t_M$, and $t_M = t_A$. The intersections of these fixed bodies will give rise to some fixed planes.

C Bosonization of the interaction on SO(7) symmetric fixed planes

For simplicity, we use the interaction Hamiltonian density on $\mathrm{SO}(7)_M$ symmetric fixed plane which is directly written in terms of Majorana operators defined in (A.7). Hamiltonian densities on the other two SO(7) symmetric fixed planes can be similarly solved via triality relation.

$$\mathcal{H}_M = g \sum_{1\leq m,n\leq 7} (i\chi_m^R\chi_n^R)(i\chi_m^L\chi_n^L) + 3(2g - t_M) \sum_{1\leq m\leq 7} (i\chi_0^R\chi_m^R)(i\chi_0^L\chi_m^L). \tag{C.1}$$

It can be rearranged into a Gross-Neveu form (up to a constant)

$$\mathcal{H}_M = -g\left(\sum_{1\leq m\leq 7} i\chi_m^R\chi_m^L + \left(3 - \frac{3t_M}{2g}\right) i\chi_0^R\chi_0^L\right)^2. \tag{C.2}$$

Therefore, when $t_M = 2g$, i.e. on the $\mathrm{SO}(7)_M$ GN fixed flow, χ_0 is decoupled in the interaction and becomes massless, corresponding to an Ising phase transition with central charge $c = \frac{1}{2}$.

According to a standard bosonization dictionary

$$i\chi_4^R\chi_4^L + i\chi_0^R\chi_0^L \sim \frac{1}{\pi a}\cos\sqrt{4\pi}\phi_{\frac{3}{2}}, \quad i\chi_4^R\chi_4^L - i\chi_0^R\chi_0^L \sim \frac{1}{\pi a}\cos\sqrt{4\pi}\theta_{\frac{3}{2}}, \tag{C.3}$$

the Hamiltonian density above can be bosonized as

$$\mathcal{H}_M = -\frac{g}{(\pi a)^2}\left(\sum_{\sigma\neq\frac{3}{2}} \cos\sqrt{4\pi}\phi_\sigma + \left(2 - \frac{3t_M}{4g}\right)\cos\sqrt{4\pi}\phi_{\frac{3}{2}} + \left(-1 + \frac{3t_M}{4g}\right)\cos\sqrt{4\pi}\theta_{\frac{3}{2}}\right)^2, \tag{C.4}$$

where in the second equality the derivative terms $-\frac{2}{\pi}(\partial_\mu\phi)^2 = (:\cos\sqrt{4\pi}\phi:)^2$ are dropped. Consider $g > 0$ case where the interactions are always relevant. For all t_M, the local minima of this bosonized Hamiltonian have ϕ_σ, $\sigma \neq \frac{3}{2}$ pinned. For $\sigma = \frac{3}{2}$, the local minima have $\phi_{\frac{3}{2}}$ pinned when $t_M < 2g$, and $\theta_{\frac{3}{2}}$ pinned when $t_M > 2g$. This also suggests that $t_M = 2g$ is an Ising transition point with central charge $c = \frac{1}{2}$. When $t_M = \frac{4}{3}g$ or $\frac{8}{3}g$, the bosonized Hamiltonian has SO(8) symmetries which is consistent with SO(8) and $\mathrm{SO}(8)_M$ fixed flows obtained from RG equations, respectively.

JHEP02(2025)202

D RG for the lattice model

We numerically integrate the RG equations on the lattice model phase diagram $P_{\mathrm{Lat}}: t_A + t_B = 0,\ t_M = -4g$. Since $u(v) = 0$ on the $v(u)$-axis, lattice model couplings u and v are related to continuum model parameters as $u = C_0(t_A + 4g)$ and $v = C_0(t_B + 4g)$. $C_0 > 0$ is an undetermined constant related to the details of coarse-graining and cutoff, which is irrelevant to our discussions. The initial values for RG equations are chosen as

$$g(0) = r_0 \cos\theta, \quad t_A(0) = -4r_0 \sin\theta, \quad t_B(0) = 4r_0 \sin\theta, \quad t_M(0) = -4r_0 \cos\theta, \tag{D.1}$$

where θ varies from 0 to 2π and $r_0 > 0$. Thus, the initial values of u and v are

$$u(0) = R_0 \cos\left(\theta + \frac{\pi}{4}\right), \quad v(0) = R_0 \sin\left(\theta + \frac{\pi}{4}\right), \tag{D.2}$$

where $R_0 = 2\sqrt{2}C_0 r_0 > 0$. Therefore, $u = v > 0$ axis, positive v-axis, negative u-axis, $u = v < 0$ axis, negative v-axis and positive u-axis are corresponding to $\theta = 0$, $\frac{1}{4}\pi$, $\frac{3}{4}\pi$, π, $\frac{5}{4}\pi$ and $\frac{7}{4}\pi$. In numerics we find a critical $\theta_c = (0.705 \pm 0.002)\pi$ for all $r_0 > 0$, such that when $0 < \theta < \theta_c$, the RG flows are controlled by the $\mathrm{SO}(8)_B$ GN fixed flow, suggesting the gapped $\mathrm{SO}(8)_B$ GN phase; when $\theta_c < \theta < \pi$ and $\pi < \theta < 2\pi - \theta_c$, the RG flows are controlled by the SO(8) GN fixed flow, suggesting the SO(8) GN phase; and when $2\pi - \theta_c < \theta < 2\pi$, the RG flows are controlled by the $\mathrm{SO}(8)_A$ GN fixed point, suggesting the $\mathrm{SO}(8)_A$ GN phase. In numerics, we locate θ_c by the sign change of t_A and t_M around it which suggests a phase transition controlled by the $\mathrm{SO}(7)_B$ GN fixed flow with central charge $c = \frac{1}{2}$. The situation of $\theta = 2\pi - \theta_c$ is similar, where the phase transition is controlled by the $\mathrm{SO}(7)_A$ GN fixed flow. When $\theta = 0$ and $\theta = \pi$, the RG flows are controlled by the G_2 TCI and the $\mathrm{SO}(7)_M$ GN fixed flows, suggesting phase transitions with central charges $c = \frac{6}{5}$ and $c = \frac{1}{2}$, respectively. Note that

$$\frac{v(0)}{u(0)} = \tan\left(\theta_c + \frac{\pi}{4}\right) \approx -\frac{1}{7}, \tag{D.3}$$

with a deviation in θ_c (with respect to 2π) less than 0.2%. This suggests that the equation of the $\mathrm{SO}(7)_B$ phase transition line is consistent with the predicted location $u = -7v$ based on a mean-field analysis. The acceptably small deviation of 0.2% arises from the perturbative nature of the one-loop RG method. By a similar argument, the $\mathrm{SO}(7)_A$ transition line is $v \approx -7u$.

Data Availability Statement. This article has no associated data or the data will not be deposited.

Code Availability Statement. This article has no associated code or the code will not be deposited.

References

[1] A.B. Zamolodchikov, *Integrals of Motion and S Matrix of the (Scaled) $T = T_c$ Ising Model with Magnetic Field*, Int. J. Mod. Phys. A **4** (1989) 4235 [INSPIRE].

[2] R. Coldea et al., *Quantum Criticality in an Ising Chain: Experimental Evidence for Emergent E_8 Symmetry*, Science **327** (2010) 177 [arXiv:1103.3694] [INSPIRE].

[3] B.A. Bernevig, J.-P. Hu, N. Toumbas and S.-C. Zhang, *The Eight-dimensional quantum Hall effect and the octonions*, Phys. Rev. Lett. **91** (2003) 236803 [cond-mat/0306045] [INSPIRE].

[4] P.L.S. Lopes, V.L. Quito, B. Han and J.C.Y. Teo, *Non-Abelian twist to integer quantum Hall states*, Phys. Rev. B **100** (2019) 085116 [arXiv:1901.09043] [INSPIRE].

[5] A. Kitaev, *Anyons in an exactly solved model and beyond*, Annals Phys. **321** (2006) 2 [cond-mat/0506438] [INSPIRE].

[6] I. Agricola, *Old and new on the exceptional group G_2*, *Not. Amer. Math. Soc.* **55** (2008) 922.

[7] J.C. Baez, *The Octonions*, Bull. Am. Math. Soc. **39** (2002) 145 [*Erratum ibid.* **42** (2005) 213] [math/0105155] [INSPIRE].

[8] Y. Hu and C.L. Kane, *Fibonacci Topological Superconductor*, Phys. Rev. Lett. **120** (2018) 066801 [arXiv:1712.03238] [INSPIRE].

[9] Z.-Q. Gao and C. Wu, *Construction of G_2 symmetry in a Hubbard-type model*, arXiv:2010.14126 [INSPIRE].

[10] Y.-M. Zhan et al., *Universal topological quantum computation with strongly correlated Majorana edge modes*, New J. Phys. **24** (2022) 043009 [arXiv:2004.03297] [INSPIRE].

[11] C. Li, V.L. Quito, D. Schuricht and P.L.S. Lopes, *G_2 integrable point characterization via isotropic spin-3 chains*, Phys. Rev. B **108** (2023) 165123 [arXiv:2305.03072] [INSPIRE].

[12] A. Rahmani, X. Zhu, M. Franz and I. Affleck, *Emergent Supersymmetry from Strongly Interacting Majorana Zero Modes*, Phys. Rev. Lett. **115** (2015) 166401 [*Erratum ibid.* **116** (2016) 109901] [arXiv:1504.05192] [INSPIRE].

[13] S.L. Shatashvili and C. Vafa, *Superstrings and manifold of exceptional holonomy*, Selecta Math. **1** (1995) 347 [hep-th/9407025] [INSPIRE].

[14] D. Friedan, Z.-A. Qiu and S.H. Shenker, *Superconformal Invariance in Two-Dimensions and the Tricritical Ising Model*, Phys. Lett. B **151** (1985) 37 [INSPIRE].

[15] Z.A. Qiu, *Supersymmetry, Two-dimensional Critical Phenomena and the Tricritical Ising Model*, Nucl. Phys. B **270** (1986) 205 [INSPIRE].

[16] Z. Bi and T. Senthil, *Adventure in Topological Phase Transitions in $3+1$-D: Non-Abelian Deconfined Quantum Criticalities and a Possible Duality*, Phys. Rev. X **9** (2019) 021034 [arXiv:1808.07465] [INSPIRE].

[17] A. Prakash, M. Fava and S.A. Parameswaran, *Multiversality and Unnecessary Criticality in One Dimension*, Phys. Rev. Lett. **130** (2023) 256401 [arXiv:2209.00037] [INSPIRE].

[18] C. Wu, J.-P. Hu and S.-C. Zhang, *Exact SO(5) Symmetry in spin 3/2 fermionic system*, Phys. Rev. Lett. **91** (2003) 186402 [cond-mat/0302165] [INSPIRE].

[19] C. Wu, *Hidden symmetry and quantum phases in spin-3/2 cold atomic systems*, Mod. Phys. Lett. B **20** (2006) 1707.

[20] M. Günaydin and S.V. Ketov, *Seven sphere and the exceptional $N = 7$ and $N = 8$ superconformal algebras*, Nucl. Phys. B **467** (1996) 215 [hep-th/9601072] [INSPIRE].

[21] R. Shankar, *Solvable Models With Selftriality in Statistical Mechanics and Field Theory*, *Phys. Rev. Lett.* **46** (1981) 379 [INSPIRE].

[22] H.-H. Lin et al., *Exact SO*(8) *symmetry in the weakly interacting two leg ladder*, *Phys. Rev. B* **58** (1998) 1794 [cond-mat/9801285] [INSPIRE].

[23] L. Fidkowski and A. Kitaev, *The effects of interactions on the topological classification of free fermion systems*, *Phys. Rev. B* **81** (2010) 134509 [arXiv:0904.2197] [INSPIRE].

[24] D.J. Gross and A. Neveu, *Dynamical Symmetry Breaking in Asymptotically Free Field Theories*, *Phys. Rev. D* **10** (1974) 3235 [INSPIRE].

[25] C. Wu, *Competing Orders in One-Dimensional Spin 3/2 Fermionic Systems*, *Phys. Rev. Lett.* **95** (2005) 266404 [cond-mat/0409247] [INSPIRE].

[26] E. Fradkin, *Field Theories of Condensed Matter Physics*, second edition, Cambridge University Press (2013) [DOI:10.1017/cbo9781139015509].

[27] M. Ninomiya and K. Yamagishi, *Nonlocal su(3) current algebra*, *Phys. Lett. B* **183** (1987) 323 [*Addendum ibid.* **190** (1987) 234] [INSPIRE].

[28] E. Ardonne and K. Schoutens, *Wavefunctions for topological quantum registers*, *Annals Phys.* **322** (2007) 201 [cond-mat/0606217] [INSPIRE].

[29] E. Grosfeld and K. Schoutens, *Non-Abelian Anyons: When Ising Meets Fibonacci*, *Phys. Rev. Lett.* **103** (2009) 076803.

[30] S.M. Girvin, *Particle-hole symmetry in the anomalous quantum Hall effect*, *Phys. Rev. B* **29** (1984) 6012 [INSPIRE].

[31] A.H. MacDonald, *Edge states in the fractional-quantum-Hall-effect regime*, *Phys. Rev. Lett.* **64** (1990) 220 [INSPIRE].

[32] C.L. Kane, M.P.A. Fisher and J. Polchinski, *Randomness at the edge: Theory of quantum Hall transport at filling* $\nu = 2/3$, *Phys. Rev. Lett.* **72** (1994) 4129 [cond-mat/9402108] [INSPIRE].

[33] P. Fendley, K. Schoutens and J. de Boer, *Lattice models with* $N = 2$ *supersymmetry*, *Phys. Rev. Lett.* **90** (2003) 120402 [hep-th/0210161] [INSPIRE].

[34] C. Li, É. Lantagne-Hurtubise and M. Franz, *Supersymmetry in an interacting Majorana model on the kagome lattice*, *Phys. Rev. B* **100** (2019) 195146 [arXiv:1811.06104] [INSPIRE].

[35] Y. Li and C. Wu, *The J-triplet Cooper pairing with magnetic dipolar interactions*, *Sci. Rep.* **2** (2012) 392.

[36] T. Grover, D.N. Sheng and A. Vishwanath, *Emergent Space-Time Supersymmetry at the Boundary of a Topological Phase*, *Science* **344** (2014) 280 [arXiv:1301.7449] [INSPIRE].

[37] Z. Pan, C. Lu, F. Yang and C. Wu, *Octupolar Weyl Superconductivity from Electron-electron Interaction*, arXiv:2411.06932.

[38] A. Bilal, *Introduction to supersymmetry*, hep-th/0101055 [INSPIRE].

JHEP02(2025)202